Correlation between resin material variables and transverse cracking in composites

SHAW MING LEE
Ciba–Geigy Corporation, Composite Materials Department, Fountain Valley, California 92708, USA

In this paper, the correlation between the resin material variables and the transverse cracking in composites is established. A theoretical model based on the fracture mechanics principle is built to describe the *in situ* failure process of transverse cracking. The central concept of the model is that the fracture is controlled by the plastic zone developed at the crack tip. Based on an approximate crack tip stress distribution, a quantitative representation is found to relate the laminate transverse cracking fracture toughness, G_c (comp), to certain resin properties: fracture toughness, G_c (resin), yield stress, σ_y, Young's modulus, E, and residual stress build-up, σ_R. G_c (comp) values of several fibre-glass/epoxy laminate systems were measured using the double torsion technique. The experimental results are found to be interpreted reasonably well by the theory. As a result, a clear picture of transverse cracking emerges. It seems that σ_y^2/E plays a more dominant role than G_c (resin) in controlling G_c (comp). The residual stress σ_R can weaken the laminate significantly when its level is high. It is also shown that the failure model discussed here can be readily applied to laminate delamination failure as well as adhesive bond fracture.

1. Introduction

Unidirectional laminates [0°] usually have poor mechanical properties in their transverse direction (90°). This poor transverse performance often carries over to the laminated composites with plies oriented in different directions. Transverse cracks parallel to the fibres in the plies are frequently induced by the applied load perpendicular to the fibre direction of the plies. The cracks usually occur at a relatively low load level, well before the full load capacity of the fibres is reached. Such damage results in laminate property degradation and, in some cases, premature laminate failure.

The macromechanical behaviour of transverse cracking has been well studied in the past [1–8]. The resin properties contributing to the failure process, however, still remain unclear due to the extremely complicated stress state in the heterogeneous fibre/matrix structure. It is well known that transverse cracking may involve both cohesive failure of the resin and adhesive fracture of the resin/fibre interface. Direct observation of a fibre glass/epoxy laminate in scanning electron microscope (SEM) by Bailey *et al.* [4] showed that transverse cracks formed by the coalescence and growth of fibre debonds. However, it has also been found [9] that transverse crack surface morphology is heavily dependent on the interfacial bonding conditions. When interfacial bond is relatively weak, debonds accompanied by a small amount of matrix cracking appear to be the major failure mode. As the interfacial bond strength increases, more matrix cracking and thus fewer fibre debonds will be present on the fracture surface. This means that cohesive failure is more likely than adhesive failure provided the fibres, perhaps with proper finishes, are well bonded to the matrix.

It is, in general, hard to distinguish the effects of cohesive and adhesive failures on the overall fracture behaviour of transverse cracking. Although transverse cracking may involve different degrees of debonding as shown in the fractographs reported in the literature (e.g. [4, 9, 10]), the
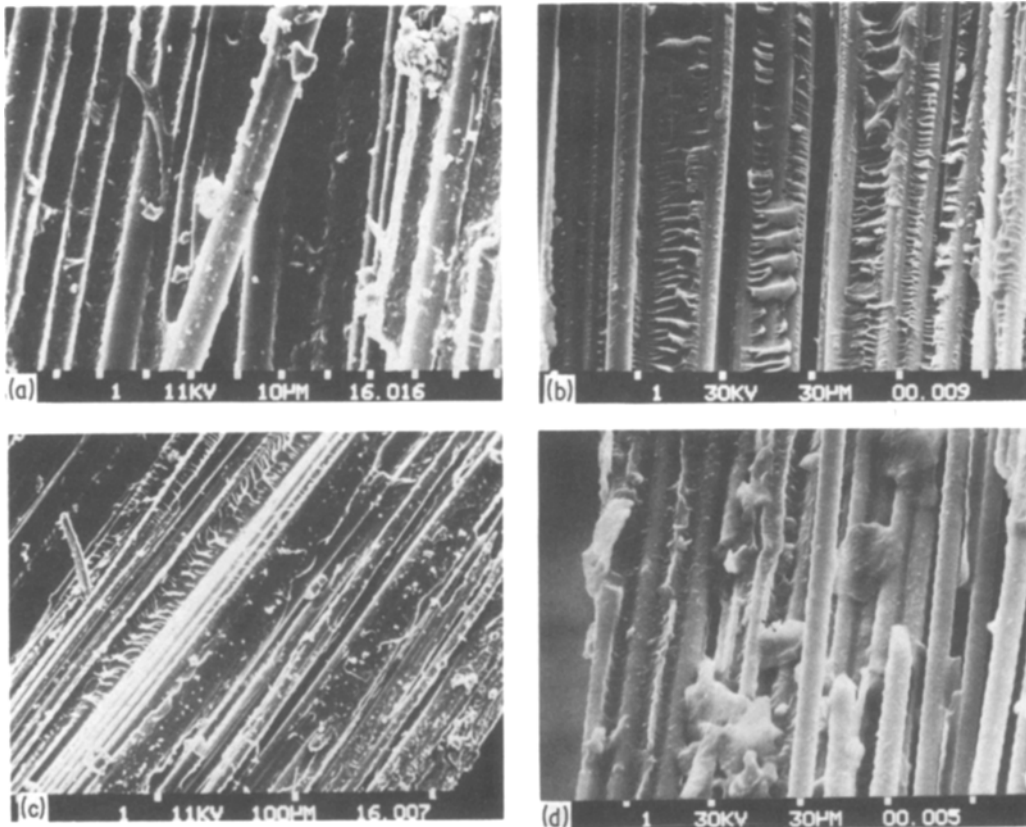
Figure 1 Scanning electron micrographs showing transverse crack surfaces of unidirectional fibre glass laminates used in this study with matrix systems of (a) 6010/972, (b) 6010/906, (c) 6010/HY 917 and (d) 6010/PACM 20/972.

matrix on the crack surface often exhibits a quite rough appearance associated with substantial plastic deformation. (This is in sharp contrast to the smooth fracture surface of a typical bulk matrix material such as epoxy.) An energetic argument given below may illustrate the importance of the matrix deformation to the failure process.

It has long been recognized from the energy principle of fracture mechanics [11, 12] that for homogeneous materials such as metals [13, 14] and polymers [15–17] the fracture energy is mostly dissipated by producing plastic flow at the crack tip. The surface energy required to create new crack surfaces by breaking chemical bonds is, actually, almost negligible compared with the plastically dissipated energy. This has been shown to be true even for very brittle materials. This important concept can be applied here to assess the relative significance of the mechanisms involved in laminate transverse cracking. The surface energy for separating adhesive fibre/matrix interfacial surfaces is expected to be

of the same order of magnitude as that for generating cohesive matrix crack surfaces [17]. The surface energy, cohesive or adhesive, involving polymers such as epoxy is estimated to be no more than $1 \, \mathrm{J \, m^{-2}}$ [15–17]. This value is certainly much smaller than the total fracture energy ($> 100 \, \mathrm{J \, m^{-2}}$) consumed by the transverse crack. The matrix plastic deformation observed on the failure surfaces should, therefore, be a major energy dissipation mechanism in the failure process. For this reason, the deformation and fracture behaviour of the resin matrix is important in controlling transverse cracking in composites.

For the glass fibre/epoxy laminate systems used in our study, transverse cracks observed in SEM are shown in Fig. 1 to have fair amount of cohesive fracture through the resin. Although some fibre debonds are observed, the matrix resin at the crack surface is shown to have undergone extensive plastic deformation. The matrix plastic deformation seen here is also quite similar to that observed in laminate delamination fracture [18]. Our attention in this study will, therefore,

Material code	Type of material	Material
6010	Epoxy resin	Diglycidyl ether of bisphenol A (DGEBA)
906	Hardener	Methyl nadic anhydride (MNA)
HY 917	Hardener	Methyltetrahydrophthalic anhydride (MTHPA)
972	Hardener	Methylene dianiline (MDA)
PACM 20	Hardener	Bis(p-aminocyclohexyl) methane (a DuPont Product)

be focused on the propagation of cohesive crack through the resin to result in crack tip plastic deformation.

In a recent paper by Lee and Schile [19] the important resin material variables controlling the transverse cracking process were studied. Two resin properties were considered to be critical: resin residual stress in the cured laminate and the fracture toughness of the resin. It was demonstrated that the residual stress build-up was much higher than what was generally speculated. It is worth mentioning that for cross-ply laminates the macroscopic thermal strains due to the heavy constraints between plies have been found [4] to have a significant effect on the laminate transverse cracking strains.

In this study, attempts are made to establish the correlation between the resin properties and the transverse cracking in composites. Laminates made from the resin systems studied earlier [19] were tested for transverse cracking fracture toughness using the double torsion technique [20]. A theoretical model based on the fracture mechanics principle is built to describe the *in situ* failure process of transverse cracking. In this model, the fracture toughness of composite is expressed quantitatively as a function of the relevant resin material variables which include those besides the resin fracture toughness and resin residual stress identified earlier. As the comparison between the experimental data and theoretical model is made, a clear picture of the resin/laminate correlation begins to emerge. As a result, the failure process of transverse cracking as well as the important resin properties are identified.

2. Experimental details
2.1. Materials description
Four Ciba—Geigy epoxy resin/hardener systems, 6010/972, 6010/HY 917, 6010/906, and 6010/PACM 20/972 studied earlier [19] were used as the matrix systems for the laminate specimens in this study. The details of the materials used are given in Table I. The stoichiometries of all the systems

and the accelerators for 6010/906 and 6010/HY 917 systems were the same as those reported in [19]. Owens—Corning S2 glass fibres (463 AA-750) were solvent (methyl ethyl ketone) impregnated with the matrix systems and wound on a drum. Unidirectional [0°] laminates (30 cm × 30 cm) of eight plies thick (∼ 1.3 mm) were made from the prepregs and cured in a press at 0.7 MPa under the curing cycles described in [19]. The resin systems all exhibited quite different flow characteristics during curing of the laminates in the press. As a result, the resin contents of the laminates were difficult to control to the same level. For each system, two laminates with different resin contents were made so that a general trend of laminate properties as a function of resin content could be observed.

2.2. Laminate fracture toughness measurement
The fracture toughness for transverse cracking of each laminate was measured by means of the double torsion (DT) test. This test has been verified recently [20] for its applicability to characterize transverse cracking by testing unidirectional [0°] laminate specimens. The laminate specimen in the DT test is a simple rectangular plate with fibres parallel to the longer axis of the specimen. The specimen supported and loaded by steel spheres, as shown in Fig. 2, is subject to a definitive four-point loading. The essential feature of the technique is that the specimen compliance, C, determined at the loading point is linearly
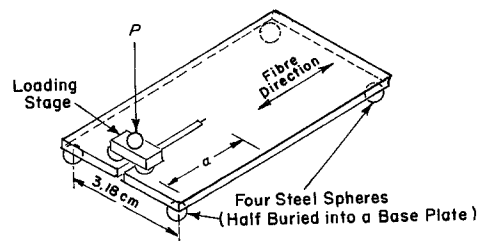

Figure 2 Schematic illustration of a double torsion test device.

related to the specimen crack length, a. In addition, the critical load, P_c, for initial crack propagation is independent of the specimen crack length, a. The composite fracture toughness, defined by the critical strain energy release rate, $G_c(comp)$, can thus be determined by

$$G_c(comp) = \frac{P_c^2}{2t} \frac{(dC)}{(da)} \qquad (1)$$

where t is the specimen thickness.

In this study, 10 to 12 DT specimens of 38.1 mm × 76.2 mm were cut from each laminate. Crack lengths ranging from 16 to 49 mm were incrementally introduced to each series of specimens. The initial notch of the specimen was introduced using a diamond saw ($\sim$ 1 mm thick) and then a fine crack was gently tapped in with a razor blade. All tests were carried out in an Instron testing machine with a crosshead speed of 0.05 cm min^{-1}. The specimen compliance, C, was determined from a plot of the inverse of the initial slope of the load, P, against deflection δ. The critical load, P_c, for crack propagation was determined by the 5% offset procedure [20–23] from the P–δ curve.

3. Theoretical model

A theoretical model is developed here based on the fracture mechanics principle to describe the possible *in situ* failure process of transverse cracking. From this model, a quantitative relation between the transverse cracking fracture toughness and the resin material properties can be established. The central concept of this theory focuses on the plastic zone developed at the crack tip as the controlling mechanism for fracture resistance. Given below are the background of this concept and the proposed *in situ* failure model.

3.1. Background
3.1.1. Neat polymer fracture
For many brittle bulk polymers, the crack propagation has been shown to be controlled by the amount of localized plastic deformation that occurs at the crack tip. For instance, a crack blunting process [24] directly related to the yield stress, σ_y, has successfully accounted for the fracture behaviour of a wide variety of epoxies. In addition, fractographic studies by Yamini and Young [25] have shown convincing evidence of the crack tip plastic zones in epoxies. The zone sizes were also found by them to be described reasonably well by

the Dugdale model [26, 27] of fracture mechanics. It has become apparent that the crack tip plastic zone dictates the fracture resistance of certain brittle polymers, especially epoxies, where there is little evidence that other possible energy absorbing mechanisms such as crazing exist.

3.1.2. Composite and adhesive bond fractures
For a transverse crack, the crack tip deformation, unlike that in a neat resin, is greatly restricted in the thin layer of resin between the closely spaced fibres. Such a constrained condition, first of all, is close to that in a delamination crack, another matrix-dominated failure mode in laminates. In addition, it is quite similar to that in an adhesive bond with resin spread between tightly spaced rigid adherends. Therefore, there are important common features between the fracture behaviour of adhesive bonds and fibre composites. Experimental evidence [28] showed that the important trends of fracture energy altering little or even increasing with decreasing temperature or increasing load rate carry over from adhesive bond fracture to delamination failure. Similar analogy is expected to exist between adhesive bond fracture and transverse cracking. Therefore, the established understanding on the adhesive bond failure can be utilized here to interpret and predict the failure process of transverse cracking in composites.

Although the exact details of crack-tip deformation have yet to be solved, recent work [29–32] did lead to a qualitative understanding about the failure behaviour of adhesive bonds. It has become clear that the plastic zone size at the crack tip is the critical parameter to determine the fracture toughness, $G_c(adhesive)$, of the adhesive bond. This concept has helped interpret the phenomenon of the dependence of $G_c(adhesive)$ on the bond thickness, h [29–32], as shown in Fig. 3. Such dependence is attributed to the increasing constraint to the crack tip deformation zone as h is decreased. The numerical results obtained by Wang *et al.* [33] on the crack tip stress distributions in a double-cantilever beam specimen are especially helpful to illustrate this effect. They found that in the adhesive layer, as the bond thickness is decreased, the stress σ_{22} ahead of a crack would decay more and more slowly than in a bulk adhesive material, as shown in Fig. 4.
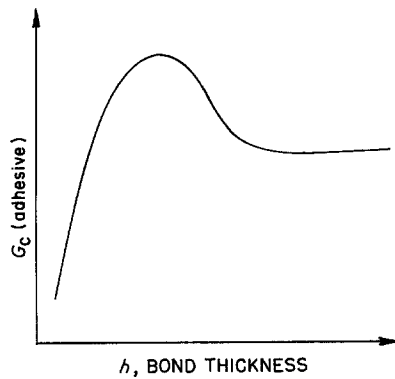
Figure 3 A typical plot of adhesive bond fracture toughness, G_c(adhesive), as a function of bond thickness.

Based on the results of Wang *et al.*, Kinloch and Shaw [32] gave a quite reasonable argument for the dependence of G_c(adhesive) on h (Fig. 3). Such dependence was qualitatively related to the plastic zone volume. At large h, the constraint to the plastic zone is negligible. The zone size as well as G_c(adhesive) are close to the values for the bulk material. As h is gradually decreased, the plastic zone would be affected by the constraints and actually elongated and increased in volume. As a result, G_c(adhesive) increases with the decrease in h. When h is decreased roughly to $2r_c$ (the diameter of the plastic zone in a bulk material) maximum value of G_c(adhesive) is achieved. The plastic zone diameter, $2r_c$, is given by [29–32]

$$2r_c = \frac{EG_c(\text{resin})}{3\pi(1-\nu^2)\sigma_y^2} \qquad (2)$$

in plane-strain condition, where G_c(resin), E, σ_y and ν are the fracture toughness, Young's modulus, yield stress and Poisson's ratio of the adhesive, respectively. For $h < 2r_c$, the constraint results in diminishing overall plastic zone volume.
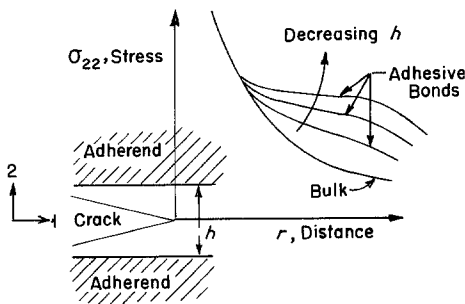
G_c(adhesive) steadily decreases as h is further reduced below $2r_c$.

The plastic zone concept, therefore, appears to provide an important insight into the failure process of adhesive joints and can be directly applied to fibre composites. Such a description of the failure behaviour is, however, still qualitative due to the lack of detailed analysis of the crack tip stress field. In our attempt to build a quantitative model here, an approximate crack tip stress field will be developed in the following section.

3.2. *In situ* failure model
3.2.1. Adhesive bond analogy

A theoretical model describing the *in situ* failure process of transverse cracking in composites is proposed here. As a first order approximation, the thin layer of resin of interest between fibres in a composite, by analogy, is replaced by a layer of resin of uniform thickness, d, between two adherends, as shown in Fig. 5. This way, the original three-dimensional problem of resin/fibre structure can be simplified to a two-dimensional problem of "equivalent" adhesive bond. The resin thickness, d, of the adhesive bond is, in principle, related to the average space between fibres. For our purpose here, it is sufficient to just assume this to be a function of resin volume content, V_R, of the laminate without further enumeration. The adherends are assumed to be of homogeneous material having the overall laminate properties. In this "equivalent" adhesive bond, a plane crack at
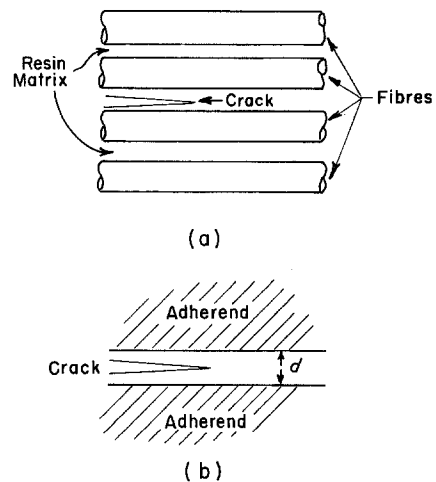

(a)

(b)

Figure 5 (a) A transverse crack in a unidirectional laminate is modelled as (b) a crack in an equivalent adhesive bond.

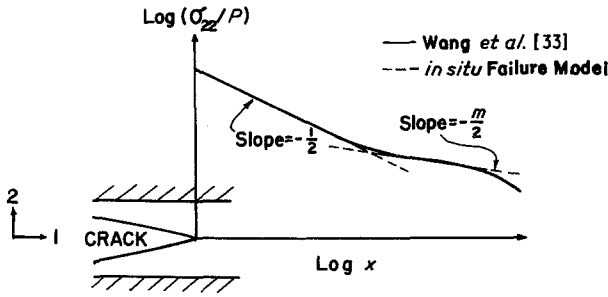*Figure 4* Effect of constraint on σ_{22} stress level ahead of a crack tip in an adhesive bond.

Figure 6 Crack tip distribution of σ_{22} along the 1-axis from Wang et al. [33] and the piecewise linear approximation in this study.

the centre of the resin (Fig. 5) is evaluated for its propagation characteristics.

The plastic zone immediately in front of a crack tip between fibres is relatively easy to occur because of the severe stress concentration at the crack tip. To develop matrix plastic deformation beyond constraining fibres, on the other hand, requires considerable deformation in the fibres to accommodate necessary matrix deformation. This is expected to be limited because the fibres are much stiffer than the resin. It is, however, possible to have matrix plastic deformation developed around fibres through a three-dimensional contour into neighbouring resin layers. For the laminates with fibre volume 60 to 70% in our study this effect may not be strong. In any case, the variations in plastic zone dimension perpendicular to the crack plane are averaged and approximated by the effective thickness of the equivalent adhesive joint proposed in our model.

3.2.2. Approximate crack tip stress distribution

The stress pattern at the crack tip is estimated here in a parametric form based on the results from Wang et al. [33]. An important finding from their study is that the conventional $r^{-1/2}$ singularity, where r is the distance from the crack tip, of stress distribution is only valid in a limited region close to the crack tip. This region was shown to be only a small fraction of the adhesive thickness. To illustrate this point, a typical log–log plot of σ_{22}/P against x, the distance from the crack tip along axis 1, is shown in Fig. 6 with P being the external load applied to the adhesive bond. Obviously, the curve is only linear with a slope of $-1/2$, meaning $r^{-1/2}$ dependence, at small x. Further away from the tip, the stress gradient is much lower than that in the $r^{-1/2}$ region. The slow varying stress state extends to a distance of several adhesive layer thickness ahead of the crack tip.

Although the numerical results from Wang et al.

[33] cannot be directly applied to our model, certain useful information can be drawn from the log–log plot of σ_{22}/P against x in Fig. 6. First of all, an important approximation can be made here to represent the curve in a piecewise linear manner. The localized region at the crack tip is represented by a straight line with a slope of $-1/2$. The region away from the crack tip with gradual decreasing stress can be fitted and represented by a straight line with a slope of $-m/2$, where $m \ll 1$ is expected. Although the numerical value of m is not immediately obvious, the physical significance of m indicated by $m \ll 1$ will become clear later. The far field stress outside these two regions is considered not significant for the crack process and is not treated here. Such a bilinear representation, although at best approximate, does serve the purpose of quantifying the stress state in order to establish the resin/composite correlation.

Based on the foregoing argument, the stress σ_{22} at the crack tip can be expressed by region of $r^{-1/2}$ dependence and region of $r^{-m/2}$ dependence, as shown in Fig. 7. With the stress profile so determined, the plastic zone length, l_p, developed at the crack tip can then be estimated by considering the region where σ_{22} is higher than the resin yield stress, σ_y. Since the dependence of σ_{22} on $r^{-1/2}$ is extremely confined to the crack tip,
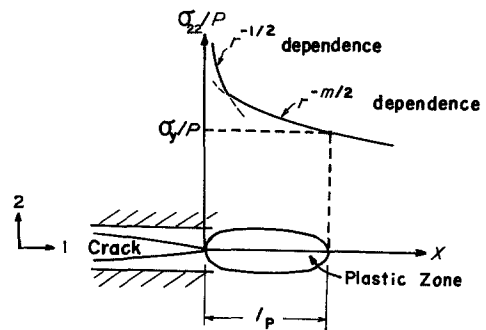

Figure 7 Schematic illustration of the plastic zone of size, l_p, developed at the crack tip in relation to the crack tip stress distribution.

2283

it can be reasonably argued that l_p extends to the region with stress of $r^{-m/2}$ dependence (shown in Fig. 7). This is a major departure from the bulk resin fracture where the crack tip plastic zone is mainly determined by the $r^{-1/2}$ dependent stress distribution.

3.2.3. Composite/resin correlation

Our attention now will focus on the macroscopically measured composite fracture toughness, $G_c(comp)$, as a function of the resin material variables involved. For ease of discussion, the contributions to $G_c(comp)$ can be differentiated into:

1. the contribution due to the resin in the absence of residual stress, defined as the neat resin contribution; and

2. the contribution due to the residual stress alone, defined as the residual stress contribution.

3.2.3.1. Neat resin contribution. At present, an ideal condition of no residual stress build-up in the laminate will be dealt with here. In a fracture toughness test, such as DT technique, the laminate specimen with a transverse crack will be under a gradually increasing load P all the way to crack propagation. The level of the crack tip stress distribution induced by a given applied load, P, is dependent on the resin modulus, E. From Wang *et al.* [33] the stress intensity factor, K_I, to P ratio was found to be proportional to $E^{1/2}$ for fixed adherend properties, or laminate properties here. σ_{22}/P in Fig. 7 being directly proportional to K_I/P would, therefore, also be proportional to $E^{1/2}$. The stress σ_{22} in the $r^{-m/2}$ dependent region of interest can be expressed by $(\sigma_{22}/P) \propto (E^{1/2}r^{-m/2})$. When the crack propagation takes place, $G_c(comp)$ can be determined from Equation 1. P_c can be related to the plastic zone length, l_p, by

$$P_c \propto (\sigma_y l_p^{m/2}/E^{1/2})$$

The (dC/da) term in Equation 1, on the other hand, is almost independent of the plastic zone for the relatively brittle failure of our interest here. (dC/da) is only related to the elastic properties of the laminate specimen involved. By combining Equation 1, and P_c, dC/da expressed above, $G_c(comp)$ can be written as

$$G_c(comp) = F\sigma_y^2 l_p^m/E \qquad (3)$$

where F is only a function of laminate elastic properties and resin volume content, V_R.

In order to relate $G_c(comp)$ to the properties of the neat resin, a failure criterion is needed to assess the critical value of l_p for crack propagation. It can be reasonably assumed that l_p is proportional to the critical plastic zone radius r_p (Equation 2) in the bulk resin, i.e.

$$l_p = Sr_p \qquad (4)$$

where S is only dependent on V_R and laminate elastic properties. $G_c(comp)$ in Equation 3 can then be rewritten as:

$$G_c(comp) = H\sigma_y^2 r_p^m/E \qquad (5)$$

where $H = FS^m$.

By substituting Equation 2 into Equation 5, $G_c(comp)$ can be found to be

$$G_c(comp) = M(\sigma_y^2/E)^{1-m}G_c^m(resin) \qquad (6)$$

where $M = H/[6\pi(1 - v^2)]^m$. Alternatively, by expressing σ_y^2/E in terms of $G_c(resin)$ and r_p, Equation 5 becomes

$$G_c(comp) = LG_c(resin) r_p^{m-1} \qquad (7)$$

where $L = H/[6\pi(1 - v^2)]$.

Equations 5 to 7 are the basic equations correlating $G_c(comp)$ with resin material variables in the absence of residual stress. The physical implication of Equation 5 is that a desired resin to resist transverse cracking should not only have large enough plastic zone size but also high enough σ_y^2/E value in the zone. It can be seen from Equation 6, expressed in terms of all measurable variables, that σ_y^2/E is at least as important as $G_c(resin)$ in contributing to $G_c(comp)$. It is also interesting to note that from Equation 7, $G_c(comp)$ increases with $G_c(resin)$ but decreases with r_p, as $m - 1 < 0$ is expected.

3.2.3.2. Residual stress contribution. The contribution from the residual stress in the resin to the composite fracture toughness will be discussed as follows. It is assumed that the crack tip stress profile in Fig. 7 with $r^{-m/2}$ dependence still holds true when the residual stress is present. Therefore, the right-hand side of Equations 6 or 7 can be considered as the invariant fracture energy term needed to propagate the crack. $G_c(comp)$, on the other hand, is the energy supplied externally, such as from a testing machine, to the failure process. In the presence of residual stress, part of the necessary fracture energy can be provided by the stored strain energy, G_R, due to the residual stress. The energy
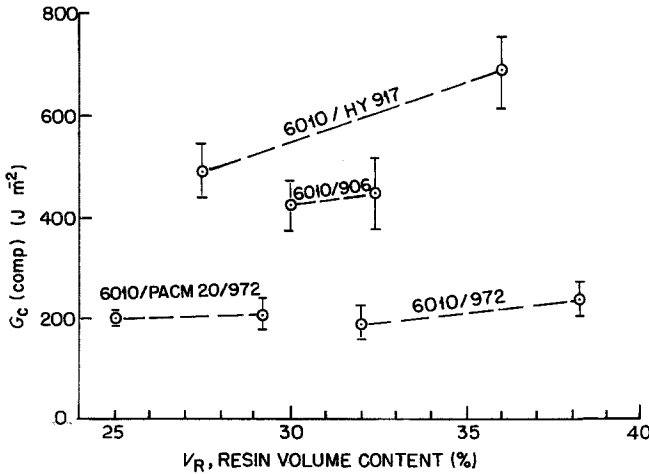
Figure 8 Measured composite fracture toughness, G_c(comp), as a function of resin volume content, V_R.

balance of this process can be found by adding G_R to the left-hand sides of Equations 6 and 7 to result in

$$G_c(\text{comp}) + G_R = L G_c(\text{resin}) \, r_p^{m-1} \qquad (8)$$

$$G_c(\text{comp}) + G_R = M(\sigma_y^2/E)^{1-m} G_c^m(\text{resin}) \quad (9)$$

G_R can be estimated by focusing on Equation 3 where G_c(comp) is expressed in terms of the σ_y^2/E in the plastic zone of size l_p. At least part of σ_y, is due to a crack tip residual stress, σ_r, term in the resin. Because of the complicated residual stress state, σ_r is defined here as an effective residual stress parameter contributing to the failure process. G_R can then be deduced from Equation 3 by replacing the term σ_y with σ_r to yield

$$G_R = F(\sigma_r^2/E) l_p^m \qquad (10)$$

The residual stress, σ_r, is difficult to estimate because a detailed residual stress distribution is simply not available. However, it can be argued that σ_r is proportional to any measurable residual stress component σ_R such as the resin hoop residual stress measured in our earlier study [19]. G_R in Equation 10 can be expressed in terms of σ_R in the form

$$G_R = N(\sigma_R^2/E) r_p^m \qquad (11)$$

where N is dependent only on V_R and laminate elastic properties.

3.2.3.3. Overall contribution. With all relevant contributions to the failure process being accounted for, G_c(comp) can be found from Equations 8 and 11

$$G_c(\text{comp}) = L G_c(\text{resin}) \, r_p^{m-1} - N(\sigma_R^2/E) \, r_p^m \quad (12)$$

or, equivalently, from Equations 2, 6, 9 and 11

$$G_c(\text{comp}) = M(\sigma_y^2/E)^{1-m} G_c^m(\text{resin})$$
$$- Q(\sigma_R^2/E) \, [E G_c(\text{resin})/\sigma_y^2]^m$$
$$\qquad (13)$$

where Q is a function of V_R and laminate elastic properties.

4. Results and discussion
4.1. Laminate fracture toughness
The fracture toughness values of the DT laminate specimens were found to be a function of resin volume contents, V_R, even within the same resin system. The G_c(comp) results are given in Fig. 8 as a function of V_R. In general, G_c(comp) gradually increases with the increased V_R. However, the rates of change of G_c(comp) with V_R have been observed to be small except for the 6010/HY 917 system. For example, for a 5% increase in V_R, G_c(comp) increases by about 7 to 15% (23% for 6010/HY 917). This effect is similar to that of the dependence of G_c on h in adhesive joints. In order to make a meaningful comparison among different resin systems, G_c(comp) of laminates with the same resin contents should be considered. For this purpose, G_c(comp) values at $V_R = 31\%$, about the medium of all the laminate resin contents, are estimated from the available data by extrapolation and given in Table II.

Our first attempt was to try to correlate G_c(comp) directly with G_c(resin). A plot of G_c(comp) against G_c(resin) is given in Fig. 9. It is obvious from Fig. 9 that the fracture toughnesses of the neat resins do not translate proportionally to those of the composites. This seems to

TABLE II Measured resin and laminate properties related to transverse cracking

Resin system	G_c(comp) at $V_R = 31\%$ (J m^{-2})	G_c(resin) (J m^{-2})	σ_y (MPa)	E (GPa)	σ_R (MPa)
6010/972	190	142	116	3.61	36.0
6010/906	420	84	115	3.21	18.0
6010/HY 917	555	144	126	3.23	71.5
6010/PACM 20/972	210	249	109	2.76	119.0

suggest that G_c(comp) is not only a function of G_c(resin). Other resin properties must also affect the transverse cracking behaviour of the laminates. This observation, however, is not all that surprising based on the argument in our model described earlier.

4.2. Application of theoretical model to experimental results

Our *in situ* failure model will be applied here to correlate the laminate fracture toughness, G_c(comp), with the resin properties. For the resin systems under our study, the resin properties of interest (G_c(resin), σ_y, E and σ_R) measured earlier [19] are given in Table II. Equation 13, being expressed in terms of all measurable variables, is focused on for discussion. The constants m, M and Q in Equation 13 are not yet analytically derivable in the absence of a detailed crack tip stress analysis. We can, however, estimate them by regression from the experimental results. All these constants are assumed to be shared by the matrix systems studied as their laminate elastic properties are comparable for fixed V_R.

To facilitate the correlation, G_c(comp) in Equation 13 can be considered as a linear function of two variables $(\sigma_y^2/E)^{1-m} G_c^m$(resin) and $-(\sigma_R^2/E) [EG_c(\text{resin})/\sigma_y^2]^m$ with constant coefficients M and Q, respectively. M and Q can,
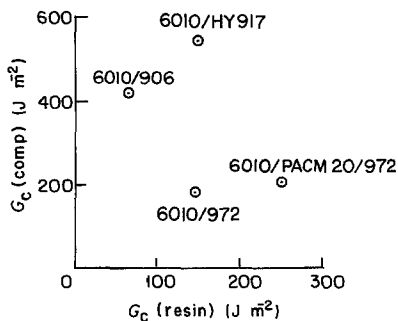
therefore, be determined by using the least square method to fit the resin and laminate properties (Table II) with Equation 13 for $m = 0$, 0.1, 0.3 and 0.7. Based on the calculated M and Q and the resin properties, estimates can be made by computing G_c(comp) from Equation 13 at fixed values of m. The estimated G_c(comp) so obtained with the corresponding values of $M(\sigma_y^2/E)^{1-m} G_c^m$(resin) and $-Q(\sigma_R^2/E) [EG_c(\text{resin})/\sigma_y^2]^m$ representing the contributions to G_c(comp) due to the neat resin and the residual stress, respectively, are given in Table III.

If the estimated values of G_c(comp) are close to the measured ones, our theory is considered reasonable in interpreting the failure process. Equation 13 then represents a reasonable quantitative resin/laminate correlation. To verify this, a comparison between the estimated G_c(comp) and measured G_c(comp) for different values of m is shown in Fig. 10. The straight line in Fig. 10 represents the ideal condition of equal estimated and measured values. It can be seen that there is a certain amount of scatter with respect to the reference line but the plot does show a notice-

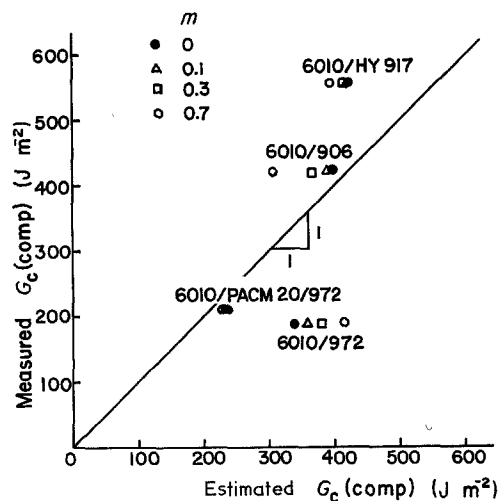*Figure 9* A plot of composite fracture toughness, G_c(comp), against resin fracture toughness, G_c(resin), for $V_R = 31\%$.

Figure 10 A comparison between the measured G_c(comp) and the estimated G_c(comp) (from Equation 13) for $V_R = 31\%$.

TABLE III Estimated laminate fracture toughness ($J\,m^{-2}$) based upon the *in situ* failure model

Matrix system	$m = 0$			$m = 0.1$			$m = 0.3$			$m = 0.7$		
	(A)	(B)	(C)	(A)	(B)	(C)	(A)	(B)	(C)	(A)	(B)	(C)
6010/972	364	−13	351	377	−15	362	400	−18	382	438	−23	415
6010/906	403	−4	399	391	−4	387	367	−4	363	313	−4	309
6010/HY 917	480	−56	424	484	−62	422	487	−73	414	481	−86	395
6010/PACM 20/972	421	−181	240	454	−216	238	524	−289	235	678	−448	230

(A) Neat resin contribution $= M(\sigma_y^2/E)^{1-m}G_c^m(\text{resin})$.
(B) Residual stress contribution $= -Q(\sigma_R^2/E)\,[EG_c(\text{resin})/\sigma_y^2]^m$.
(C) Laminate fracture toughness $= G_c(\text{comp})$.
(C) = (A) + (B) (see Equation 13).

able relation between estimates and measurements. The scatter appears to decrease as m approaches zero. This is quite reasonable since $m \ll 1$, as shown in Fig. 6, is expected. The estimated $G_c(\text{comp})$ of all the systems except 6010/972 are reasonably close to the experimental values. The scatter may result from the assumption of the same constants m, M and Q for all the systems. Strictly speaking, laminate elastic properties and thus these constants are expected to vary, at least slightly, from system to system. In view of the simplified assumptions made in our theoretical model, the comparison above seems to indicate that the model does give a reasonable interpretation of the failure process. Moreover, the important resin material variables controlling transverse cracking are identified.

A clear picture of transverse crack propagation in laminates now emerges. It appears that the plastic zone at the crack tip dominates the failure process. The fracture resistance of the laminates is mainly controlled by (a) the neat resin properties, $G_c(\text{resin})$, σ_y and E, as well as (b) the resin residual stress, σ_R, in the laminate. It has been shown that for the laminates of 31% resin content examined here the contribution to $G_c(\text{comp})$ from the neat resin seems to be a strong function of the σ_y^2/E. The $G_c(\text{resin})$, in contrast, appears to be less important as can be seen from the weak $G_c^m(\text{resin})$ dependence in Equation 13 where m is small. Although the exact value of m cannot be deduced, it can be seen from Fig. 10 that the estimated $G_c(\text{comp})$ alters little when m varies in the range of $0 < m < 0.3$. For ease of discussion, $m = 0.1$ is assumed here.

It is interesting to observe the effect of σ_y^2/E with respect to $G_c(\text{resin})$ in contributing to $G_c(\text{comp})$. For instance, 6010/972 and 6010/HY 917 systems with almost the same values of $G_c(\text{resin})$ have their neat resin contributions 377 and $484\,J\,m^{-2}$ at $m = 0.1$, respectively. This

difference mainly results from their different σ_y^2/E values. Also, the system 6010/PACM 20/972 with the highest $G_c(\text{resin})$ among all the systems has only a neat resin contribution of $454\,J\,m^{-2}$ at $m = 0.1$ because of its relatively low σ_y^2/E.

The residual stress contribution to $G_c(\text{comp})$ is also quite significant. The fairly low residual stress build-up of the system 6010/906 has little effect on $G_c(\text{comp})$. As our model shows that $G_c(\text{comp})$ is a function of σ_R^2/E (e.g. Equation 13), the residual stress contribution increases rapidly with the increase in σ_R. This is pronounced for the 6010/PACM 20/972 system where the residual stress contribution ($216\,J\,m^{-2}$) is almost half of the neat resin contribution ($454\,J\,m^{-2}$). The implication is that in a laminate a severe residual stress build-up could significantly offset the toughening effect gained from the neat resin.

The argument presented in this study for transverse cracking in composites can, in principle, be applied to adhesive bond failure as well as interlaminar delamination failure in composites. After all, the model proposed here is based on an "equivalent" adhesive bond concept. Besides, the delamination crack in the thin resin layer between laminae in a laminate is quite similar to the adhesive bond and can be described by the same model proposed in this study. For example, the observed $G_c(\text{adhesive})$ [30] and $G_c(\text{delamination})$ [28] which altered little or even increased with decreasing temperature or increasing loading rate, can be accounted for by our model. For general polymers, when temperature decreases or loading rate increases, $G_c(\text{resin})$ will usually drop, but σ_y^2/E may actually go up. $G_c(\text{adhesive})$ or $G_c(\text{delamination})$, being a stronger function of σ_y^2/E than of $G_c(\text{resin})$, may also increase. Such observations further support our concept and manifest the important resin properties in controlling the fracture of composites or adhesive bonds.

5. Conclusions

In this study, the correlation between the resin material variables and transverse cracking of composites is established. A theoretical model is built to describe the *in situ* failure process of transverse cracking. The experimental results compared with the theoretical model yield important information of the failure mechanism of transverse cracking as well as the important resin material properties controlling cracking. An important finding is that the resin yield stress, σ_y, and Young's modulus, E, along with the resin fracture toughness, G_c(resin), control the fracture toughness of the composites. The residual stress build-up can significantly weaken the transverse cracking resistance of the laminates. At least for the fibre glass laminates studied here, such evidence is strong.

Although the theoretical model is based on simplified assumptions, the physical implications indicated by Equations 12 and 13 in this model are quite sound. The model, of course, is subject to further modification when a better micromechanical stress analysis becomes available. The model is shown to be also applicable to laminate delamination failure and adhesive bond fracture. The resin controlled failures in both laminates and adhesive bonds, therefore, become better understood as a result of this study.

References

1. K. W. GARRETT and J. E. BAILEY, *J. Mater. Sci.* **12** (1977) 157.
2. A. PARVIZI, K. W. GARRETT and J. E. BAILEY, *ibid.* **13** (1978) 195.
3. A. PARVIZI and J. E. BAILEY, *ibid.* **13** (1978) 2131.
4. J. E. BAILEY, P. T. CURTIS and A. PARVIZI, *Proc. Roy. Soc.* **A366** (1979) 599.
5. M. G. BADER, J. E. BAILEY, P. T. CURTIS and A. PARVIZI, Proceedings of the 3rd International Symposium on the Mechanical Behaviour of Materials, Cambridge, UK, 20–24 August 1979 (Pergamon Press, Oxford, UK, Elmsford, New York (1980) Vol. 3, p. 227.
6. A. S. D. WANG and F. W. CROSSMAN, *J. Comp. Mater. Suppl.* **14** (1980) 71.
7. F. W. CROSSMAN, W. J. WARREN, A. S. D. WANG and G. E. LAW, JR, *ibid.* **14** (1980) 88.
8. D. L. FLAGGS and M. H. KURAL, *J. Comp. Mater.* **16** (1982) 103.
9. C. C. CHAMIS, "Composite Materials", Vol. 6, edited by L. J. Broutman and R. H. Krock (Academic Press, New York, 1974) pp. 40–3.
10. B. HARRIS, *Met. Sci.* **14** (1980) 351.
11. J. F. KNOTT, "Fundamentals of Fracture Mechanics" (Halsted Press, New York, 1973) p. 110.
12. D. BROEK, "Elementary Engineering Fracture Mechanics" (Sijthoff and Noordhoff, The Netherlands, 1978) 119–20.
13. E. OROWAN, *Trans. Inst. Eng. Shipbuilders Scotland* **89** (1945) 165.
14. G. R. IRWIN, 9th International Congress on Applied Mechanics, VIII, Paper 101(II), University of Brussels (1957) p. 245.
15. R. J. YOUNG, "Development in Polymer Fracture – 1", edited by E. H. Andrews (Applied Science Publishers, London, 1979) pp. 184–8.
16. I. M. WARD, "Mechanical Properties of Solid Polymers" (Wiley, New York, 1971) pp. 341–8.
17. B. W. CHERRY, "Polymer Surfaces" (Cambridge University Press, Cambridge, UK, 1981).
18. W. D. BASCOM, J. L. BITNER, R. J. MOULTON and A. R. SIEBERT, *Composites* **11** (1980) 9.
19. S. M. LEE and R. D. SCHILE, *J. Mater. Sci.* **17** (1982) 2095.
20. S. M. LEE, *J. Mater. Sci. Lett.* **1** (1982) 511.
21. J. F. KNOTT, "Fundamentals of Fracture Mechanics" (Halsted Press, New York, 1973) p. 140.
22. D. BROEK, "Elementary Engineering Fracture Mechanics" (Sijthoff and Noordhoff, The Netherlands, 1978) p. 175.
23. J. T. BARNBY and B. SPENCER, *J. Mater. Sci.* **11** (1976) 78.
24. A. J. KINLOCH and J. G. WILLIAMS, *ibid.* **15** (1980) 987.
25. S. YAMINI and R. J. YOUNG, *ibid.* **15** (1980) 1823.
26. J. F. KNOTT, "Fundamentals of Fracture Mechanics" (Halsted Press, New York, 1973) p. 69.
27. D. BROEK, "Elementary Engineering Fracture Mechanics" (Sijthoff and Noordhoff, Amsterdam, 1978) p. 96.
28. D. L. HUNSTON, W. D. BASCOM and J. L. BITNER, Abstracts of the papers presented at the 5th Annual Meeting of the Adhesion Society, Mobile, Alabama, 22–24 February (1982) Abstract 17a–17c.
29. W. D. BASCOM, R. L. COTTINGTON, R. L. JONES and P. PEYSER, *J. Appl. Polymer Sci.* **19** (1975) 2545.
30. W. D. BASCOM and R. L. COTTINGTON, *J. Adhes.* **7** (1976) 333.
31. D. L. HUNSTON, J. L. RUSHFORD, J. L. BITNER, J. OROSHNIK and W. S. ROSE, *J. Elastomers Plast.* **12** (1980) 133.
32. A. J. KINLOCH and S. J. SHAW, *J. Adhes.* **12** (1981) 59.
33. S. S. WANG, J. F. MANDELL and F. J. McGARRY, *Int. J. Fract.* **14** (1978) 39.